

## Behaviour of lightweight composite trusses in fire – A case study

Seng-Kwan Choi<sup>†</sup>

*Department of Fire and Engineering Service Research, Korea Institute of Construction Technology,  
Ilsan, Goyang 411-712, Korea*

Ian Burgess

*Department of Civil and Structural Engineering, University of Sheffield, Mappin Street,  
Sheffield S1 3JD, UK*

Roger Plank

*School of Architecture, University of Sheffield, Western Bank, Sheffield S10 2TN, UK*

*(Received August 16, 2006, Accepted December 15, 2006)*

**Abstract.** On September 11<sup>th</sup> 2001, the twin towers of the World Trade Center in New York City were struck by two hijacked airplanes. Despite severe local damage induced by the impact, the towers were able to sustain 102 and 56 minutes of the subsequent multi-storey fires before collapsing. The purpose of this study is to contribute to the understanding of the in-fire performance of composite trusses by examining the behaviour of the longer-span type used in the towers. It makes no attempt to be a forensic study of the actual events. Using the finite element package Vulcan, the structural mechanics of typical long-span composite floor trusses are explained, under a variety of scenarios, as the fire temperatures rise. Different boundary conditions, degrees of protection and loading are all covered, the results being presented mainly in the form of graphs of deflection and internal force of members against time.

**Keywords:** composite truss; catenary action; numerical modelling; progressive collapse; structural fire engineering; World Trade Center.

---

### 1. Introduction

The collapse of the North Tower of the World Trade Center (WTC 1) was initiated at 8:45 am on September 11<sup>th</sup> 2001 by the strike of a hijacked Boeing 767-200ER on the north face of the tower between the 94th and 98th of its 110 floors. Significant damage to partition walls in the occupancy floor and partial collapse of frames in the steel-framed core were reported by occupants of floors directly below the impacted area (Federal Emergency Management Agency 2002). Consequently, the one-way

---

<sup>†</sup>Corresponding Author, E-mail: [sengkwanchoi@kict.re.kr](mailto:sengkwanchoi@kict.re.kr)

acting, long-span composite floors, which spanned between the core and these perimeter columns in the impact zone, were also damaged over large areas. Some debris from the plane, which penetrated through the building, was found in nearby buildings and streets. At 9:06 am, another hijacked Boeing 767-200ER struck the south face of the South Tower (WTC 2) at a skewed angle, impacting between the 78<sup>th</sup> and 84<sup>th</sup> floors. It has been assumed that the pattern of structural damage caused to the perimeter frame, core and floors of this tower may have been similar to that experienced by WTC 1. However, given the much more skewed impact direction, the off-centre location and the 90° difference in alignment of the cores of the two towers, in this case it is possible that more damage may have been caused to the two-way spanning corner floor system as well as the one-way spanning short-span floors directly behind the impact zone.

Immediately after WTC 2 was struck it was observed that large-scale fireballs, forming from the dispersion of the jet fuel from the plane, emanated through broken windows and frames to three sides of the impact area in the tower. The internal conflagrations which caused these fireballs are believed to have ignited very severe fires over the combustible surfaces within the tower during a short period, and accompanying smoke was observed from these areas. No explosion was reported during the period of fire. Less information regarding the initial fire in WTC 1 is available, but it is believed that the sequence followed a fairly similar pattern. The towers had originally been designed against the impact of a Boeing 707 (Fitzpatrick, Crane and Rajii 2002/winter) and were constructed with a high degree of built-in redundancy. Through the load redistribution which can occur under such conditions, WTC 1 and WTC 2 managed to sustain 103 and 56 minutes respectively of the ensuing fires before collapse ensued.

The following study was developed as a contribution to the understanding of the structural performance of WTC 1 during the fire. Unlike a typical compartment fire study, this case contains many uncertainties such as details of the damage caused by the airplane impact to the floor structure, the removal of fire-proofing material on exposed steelwork, and the scale and intensity of the fire which certainly involved simultaneous burning on significant areas of several floors in and around the impact zone. Whilst making various assumptions to simulate extreme situations encountered during the event, the study was conducted to investigate numerically the behaviour of the composite truss.

## **2. Modelling**

Both of the twin towers were 110-storey steel-framed buildings, each storey having a square footprint of approximately 3980 m<sup>2</sup> (63.7 m × 63.7 m). The perimeter of each building consisted of an array of fabricated square steel box-columns of 356 mm side length, spaced at 1.0 m centres, which were linked at each floor level by a 1.3 m deep spandrel girder to form a vertical Vierendeel grillage on each face of the building. Various strengths and thicknesses of steel plate were used for the perimeter columns, depending on their location. The central core (26.2 m × 42.3 m) of the building comprised an array of larger box or wide-flange-section columns, at greater spacing, clad with lightweight dry-wall panelling as insulation to the elevators, escalators, emergency stairways and services housed in the core. A typical occupancy floor was supported by parallel one-way spanning composite trusses, on two sides having 18.3 m span and on the other two having 10.7 m span. These composite trusses spanned from the core area, in pairs, to alternate perimeter columns of the building. In the four 18.3 m × 10.7 m corner areas, a two-way spanning grillage of trusses was used.

In the long-span areas, one of which was the immediate area of impact in WTC 1, pairs of composite trusses were used, which were 18.3 m long, 752.8 mm deep and at 2.0 m spacing, supporting a concrete



### 3. Temperature assessment

The Federal Emergency Management Agency (2002) has estimated that approximately 4000 gallons of airplane fuel may have remained on the impacted floors of WTC 1. If this is assumed to have been evenly distributed over five damaged floors in WTC 1, the increase of the fire load due to the fuel would not have been significantly different from a generic fire load in the office space (European Committee for Standardisation 1991). However, as jet fuel is volatile, it is believed that it must have induced the spontaneous spread of fire to combustible surfaces over these floors at an early stage of the fire.

Determination of the ‘opening factor’ is dependent on the aircraft impact damage, which varied between the floors. However, in all cases this was relatively low due to the large ratio of floor area to storey height. For these reasons, the standard ISO834 fire (International Organization for Standardization 1975) was adopted in order to assess the temperature development of the composite truss. The influence of an active sprinkler protection system was not included, since this is believed to be certainly inactive or ineffective under such an observed explosive spread of fire situation (Federal Emergency Management Agency 2002). The insulation of the long-span composite trusses in both WTC towers was designed (using a prescriptive method (Milke 2003)) to resist two hours of the standard fire under normal conditions. Due to the airplane impact and blast, very little of the extremely fragile sprayed insulation material would have remained intact on the sprayed surfaces of many truss members. Hence, this study considered both fully protected and unprotected composite trusses, in order to achieve reasonable upper and lower bound representations of the situation. The column was assumed to remain protected in both of the cases.

For the unprotected case, the temperature development of each of the chord members (Fig. 2) was calculated on the basis of the section factor,  $(A/V)$ , using a formula provided by Eurocode 4 Part 1.2 (European Committee for Standardisation 1994). The temperature increase,  $\Delta\theta_a$ , of unprotected steel chords during the time interval,  $\Delta t$ , may be determined by following formula:

$$\Delta\theta_a = \frac{\alpha_c + \alpha_r}{C_a \rho_a} \cdot \frac{A}{V} \cdot (\theta_i - \theta_a) \cdot \Delta t \quad (1)$$

where the coefficient of radiative heat transfer,  $\alpha_r$ , is given by:

$$\alpha_r = \Phi \left( \frac{5.67 \times 10^{-8} \varepsilon_{res}}{\theta_i - \theta_a} \right) ((\theta_i + 273)^4 - (\theta_a + 273)^4) \quad (2)$$

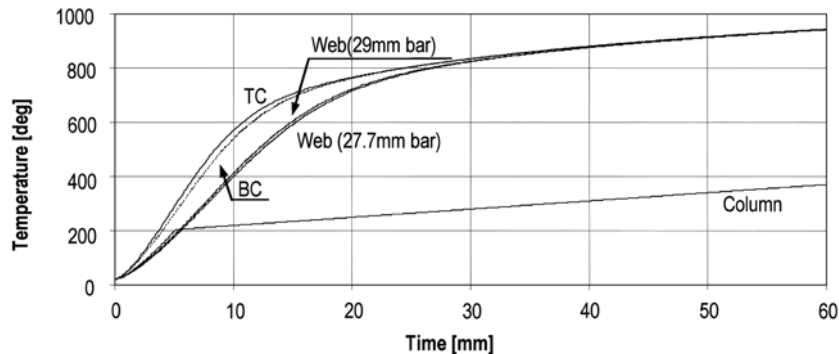


Fig. 2 Temperature development of unprotected chord members in the standard fire

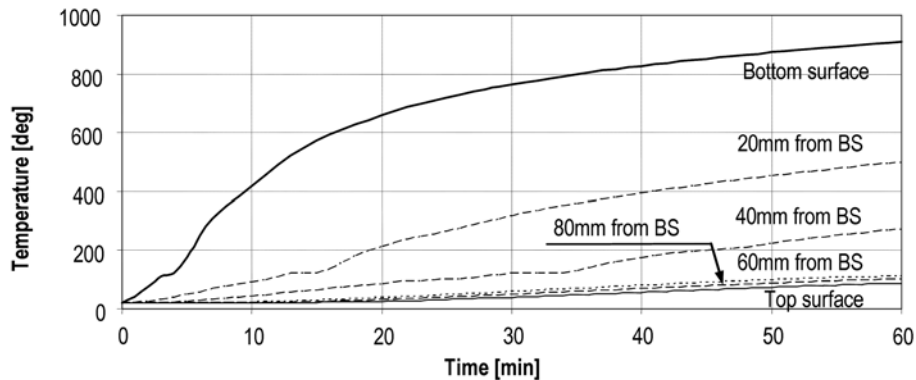


Fig. 3 Temperature development of 100mm topping of LWC slab in the standard fire

Typically, steelwork insulated by means of an intumescent coating exhibits a similar temperature development to that of unprotected steelwork up until the point at which the coating ‘activates’ (generally around 200 °C, although this may vary). Therefore, for the protected truss case, the temperature development of the chord members was assumed to increase to about 200 °C in accordance with Eq. (1) and (2) and then progress linearly up to 620 °C at 120 minutes for both top and bottom chords, and to 550 °C for web members.

A thermal analysis (Fig. 3) was conducted using heat transfer software (Huang *et al.* 1996), to generate the temperature development of the LWC slab topping, which was divided into 9 layers, in the standard fire. The moisture content was taken to be 2.0 % of the concrete weight and coefficients of heat transfer were chosen from generic data given by Purkiss (1996).

#### 4. Material properties at elevated temperature

The performance of concrete and steel varies progressively at elevated temperatures, with temperature-dependent variation of characteristics such as strength, stiffness, thermal expansion, specific heat, and thermal conductivity. For numerical analyses, the thermal characteristics of the materials were formulated in accordance with Eurocode 3 Part 1.2 (European Committee for Standardisation 1993) and Eurocode 4 Part 1.2 (European Committee for Standardisation 1994).

The stress-strain relationship of the steel at elevated temperatures was assumed to be in accordance with Eurocode 3, as shown in Fig. 4. The set of linear-elliptical curves, excluding strain hardening, assumes that the yielding initiates at a 2 % strain limit at any temperature, and that the ultimate strain is defined at a 20 % strain limit. This is assumed to be identical under both compressive and tensile stress conditions. The constitutive model implies also rules for reverse-straining (“unloading”) from plastic strain states. It is noted that the steel begins to lose a significant amount of its strength at the 2 % strain limit at temperatures above 400 °C, with approximately 11 % of its strength remaining at 800 °C. The yield stress was assumed to be zero at 1200 °C for design purposes.

Due to the heterogeneous nature of concrete, as a mixture of cement paste, sand, aggregate of different types, small quantities of additions, both chemically-bound and free water, and pore structures, it is difficult to establish accurate temperature-dependent characteristics. The stress-strain relationship of lightweight concrete in compression over the range of elevated temperatures used for this study is

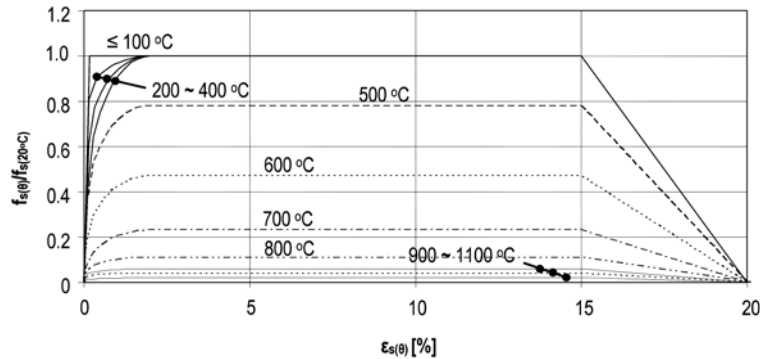


Fig. 4 Stress-strain relationship of steel at elevated temperatures

shown in Fig. 5. Lightweight concrete has a lower decrease of strength and stiffness at elevated temperatures, due to the low thermal conductivity of lightweight aggregate compared to that of normal aggregates (Neville 1998). The tensile strength of the concrete at elevated temperatures was taken into account by adopting a tensile stress-strain curve, proposed by Rots *et al.* (1984) and tested by Huang and Plattern (1997) & Jun *et al.* (2003). The curve, shown in Fig. 6, was modelled as linear behaviour up to the peak tensile strength,  $f_t(\theta) = 0.3321 \sqrt{f_c}(\theta)$  (American Society of Civil Engineering 1984), which does not exceed 10 % of the corresponding compressive strength suggested by Eurocode 4 Part 1.2 (European Committee for Standardisation 1994). Beyond this strain a bilinear curve for tensile strain-softening after cracking was assumed (Barzegar-Jamshidi 1987), up to the maximum tensile strain  $\varepsilon_{ct}(\theta) = 1.5f_t(\theta)/E_c(\theta)$ . After cracking under tension the concrete is still able to carry compression, but after crushing in compression all strength is lost.

## 5. Parametric studies

The numerical analyses of the structural behaviour of the long span floor system of WTC 1 in fire were conducted using the finite element program Vulcan, which has been specifically developed by the Structural Fire Engineering Group at the University of Sheffield (Najjar 1994, Bailey 1995, Shepherd

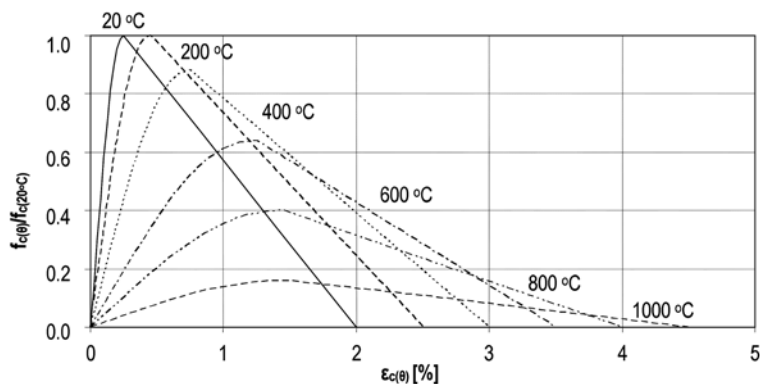


Fig. 5 Stress-strain relationship of concrete in compression at elevated temperatures

1999, Cai 2003 and Huang *et al.* 2003a&b) to investigate structural performance at elevated temperatures. The composite truss was modelled using two- and three-noded segmented 3D beam-column elements, an approach which allows the cross section to contain as many segments, allocated to steel, concrete or vacant space, as are needed for accuracy, and so it is possible to model any shape and material combination. The Newton-Raphson technique is employed for the solution procedure to obtain the load-deformation characteristics of the structures at each increment of temperature or load.

### 5.1. The unrestrained composite truss

After the attack on WTC 1, it was observed that significant numbers of the external columns were damaged or cut due to the crash. Furthermore, several floors were simultaneously exposed to fire caused by the widely-spread jet fuel. In this situation, the top and bottom floors of this part of the structure may still retain the restraint to horizontal movement provided by the supporting column. However it is likely that, on the intermediate floors, the columns will have provided little horizontal reaction. In order to understand the behaviour of these intermediate floors in fire, a simply supported composite truss, both with and without protection, was numerically analysed using Vulcan for 60 minutes of the standard fire, under loadings of 4.8 kN/m<sup>2</sup> at the fire design limit state and 3.9 kN/m<sup>2</sup> under the arbitrary condition.

The equilibrium configuration of the composite truss at ambient temperature is illustrated in Fig. 7. Double-ended black- and white-filled arrows indicate resultant compression and tension respectively. Single-ended black-filled vertical arrows represent resultant shear forces. The critical elements of the model can be identified at ambient temperature by examining the load ratios in the members. The peak value of load ratio under tension occurs in the mid-span member of the bottom chord, 8.5 to 9.0 m from the support. In terms of compression it is the second compressive web member, which is the fourth web member from the support.

The results of the numerical analyses of the protected and unprotected composite trusses are shown in terms of their vertical mid-span deflections against time, in Fig. 8. The protected composite truss, under the loadings of 4.8 kN/m<sup>2</sup> and 3.9 kN/m<sup>2</sup>, deflects by approximately L/100 and L/150 respectively after 60 minutes of the standard fire. During this period the flexural action of the protected models is maintained without any local instability. The unprotected trusses resist heating up to 12.5 and 13.4 minutes respectively, at which times the second compressive web members buckle in each case due to the rapid temperature increase of the unprotected web members in the early stages of the standard fire. The bottom chord temperatures reach 572 °C (with a strength retention factor of 0.56 at the 2.0 % strain

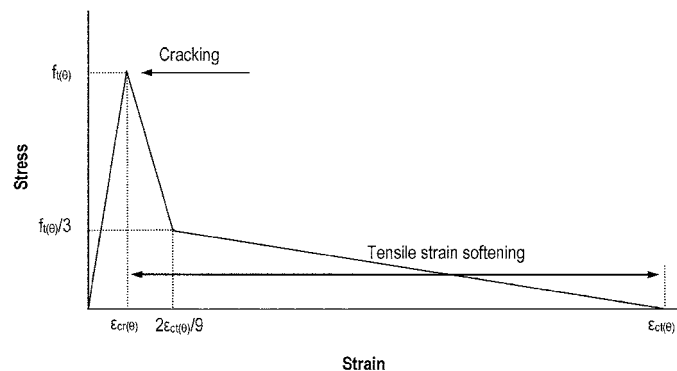


Fig. 6 Stress-strain relationship of concrete in tension at elevated temperatures

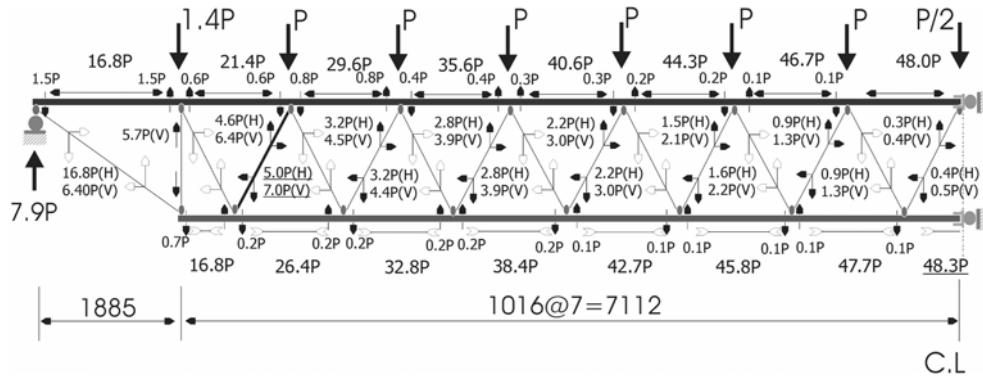


Fig. 7 Equilibrium of the unrestrained composite truss at ambient temperature

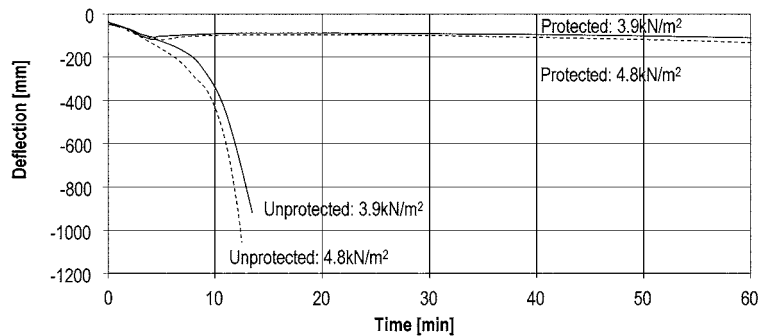


Fig. 8 Vertical deflection of the mid-span of the top chord in the standard fire

limit (European Committee for Standardisation 1993)) and 630 °C (with strength retention of 0.40). Fig. 9 shows results for the case of an unprotected composite truss with loading of 4.8 kN/m<sup>2</sup> (where 'BC #' or 'TC #' respectively denotes the top and bottom chord forces at panels from the support to the mid-span of the truss). It is clear that, variation along the z-axis, of the top and bottom chords in the unprotected composite truss under a loading of 4.8 kN/m<sup>2</sup> is shown to be maintained solely in compression and tension respectively during the fire resistance period. This observed trend illustrates represents that the flexural mechanism of the model is thoroughly maintained until the occurrence of the local instability.

Indeed, it is the instability of individual web members that initiates failure of the system by preventing it from acting in flexure. Hence, for the levels of loading considered and for simply supported conditions, the fire protection level of these critical web elements is the most important factor in determining the structural resistance of the system in a standard fire. The unprotected condition can, in this case, also be used to simulate a moderate level of structural damage to a fully-protected truss. A similar pattern of behaviour was observed for more general composite truss configurations in fire (Choi 2005).

## 5.2 The composite truss with a supporting column

To simulate the top and bottom floors in the fire-exposed levels, or floors in a localised compartment fire, the structural behaviour of protected and unprotected composite trusses with a supporting column

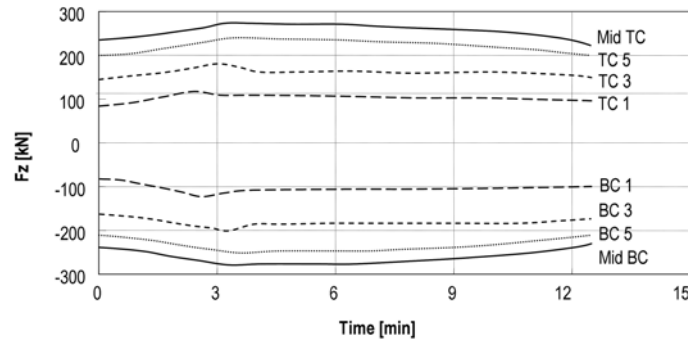


Fig. 9 Internal force variation along z-axis in top and bottom chords

was numerically investigated over 60 minutes of the standard fire. Again, this was carried out using Vulcan and loading of both  $4.8 \text{ kN/m}^2$  and  $3.9 \text{ kN/m}^2$ . Once more, the performance of the models is shown, in Fig. 10, in terms of the vertical deflection of the mid-span top chord against time. In order to illustrate the contribution of the supporting column to the behaviour of the composite truss in fire, the variation of the horizontal reaction at the beam-column connection is plotted in Fig. 11.

Fig. 10 shows that the protected models are able to resist 60 minutes of the standard fire with a deflection no greater than  $L/90$ . During this period, the flexural action is maintained (Fig. 12(a)) as it is in the unrestrained condition. Hence, the supporting column consistently experiences a push-out force (Fig. 11) due to the thermal elongation of the slab and top chord. Since the model under the lower loading level naturally deflects less than that with the higher loading, rotation at the support is lower and any thermal elongation tends to occur more in the horizontal direction (along the z-axis). This situation, when coupled with a restrained end condition, induces the development of higher horizontal axial forces with increasing temperatures in the less loaded model while the load-carrying mechanism is predominantly bending.

Fig. 10 also indicates that, for both of the loading scenarios, the unprotected models experience their first member instability at 17.0 and 18.0 minutes of the standard fire. It can be seen in Fig. 11 that, for the model under  $4.8 \text{ kN/m}^2$  loading, the horizontal reaction force at the support changed from push-out to pull-in at 10.9 minutes of standard fire exposure, before the occurrence of any local instability. This change shows the transition of the load-carrying mechanism of the structural system from one in which

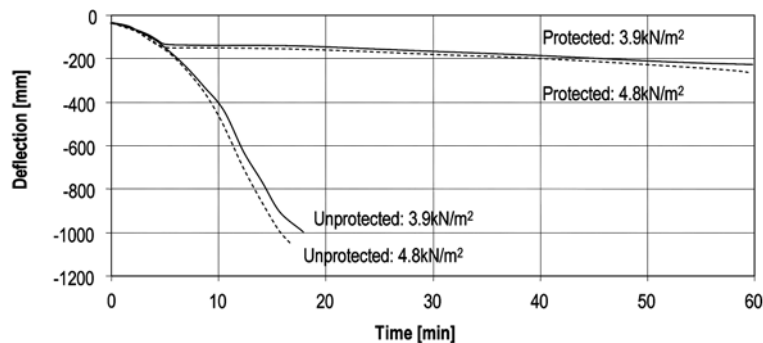


Fig. 10 Vertical deflection at the mid-span of the top chord in the standard fire

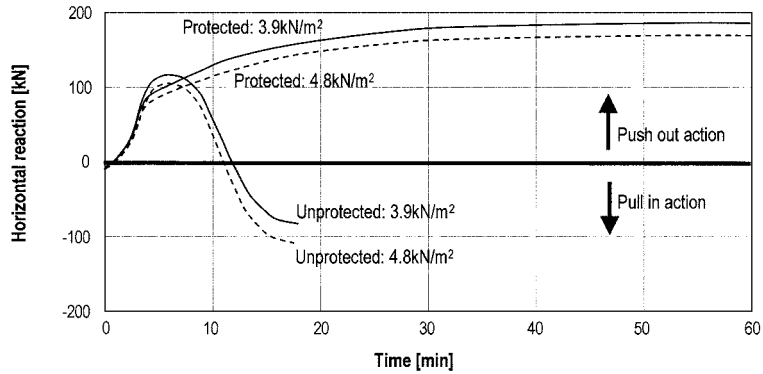


Fig. 11 Horizontal reaction at the beam-column connection in the standard fire

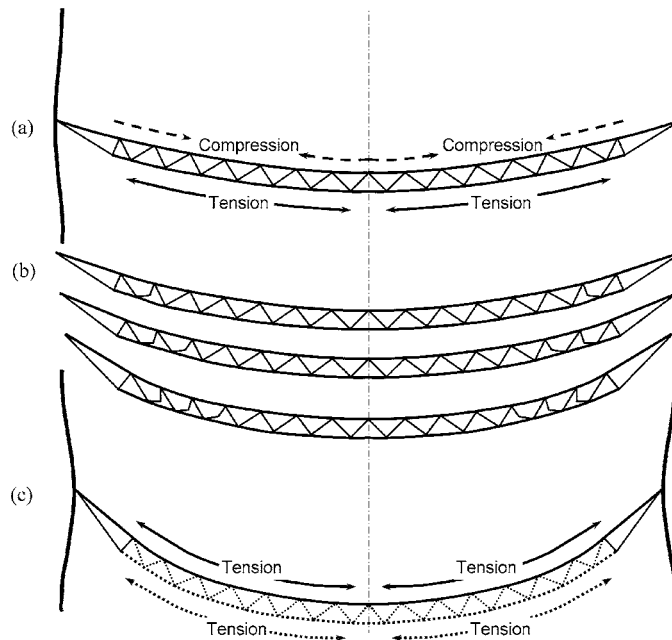


Fig. 12 Structural mechanism of the composite truss in fire: (a) in bending; (b) as diagonals buckle progressively (but almost at the same instance); (c) in full catenary action

restraint resists a net expansion to where thermal curvature due to differential expansion of top and bottom chords dominates the response. With this in mind, and in order to determine the contribution of each member group (bottom chord, top chord plus slab and web members) to the in-fire global performance in more detail, the contribution to the internal force redistribution of each group was firstly determined. Fig. 13 shows the force redistribution in the bottom chord, this particular plot being of the greatest interest, as the deflection pattern of a composite truss is generally governed by the integrity of this element. Plots for the top chord and slab and finally the web members are shown in Fig. 14 and 15 respectively.

At 8.3 minutes of the fire, the temperature of the bottom chord reaches  $456\text{ }^{\circ}\text{C}$  and the mid-span section becomes fully plastic in terms of flexural capacity at the 2.0 % strain limit. Once this has

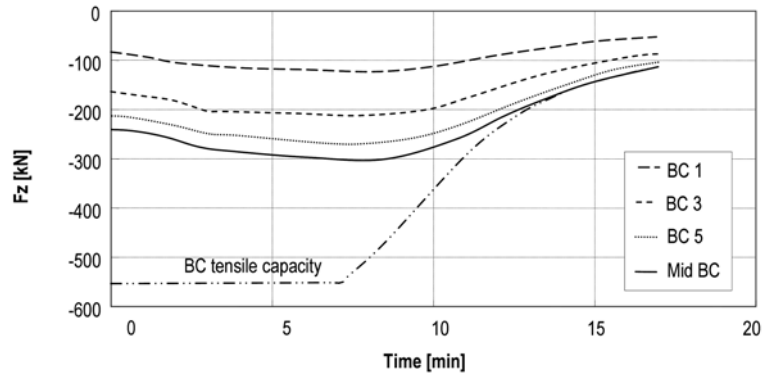


Fig. 13 Internal force variation along z-axis in bottom chord

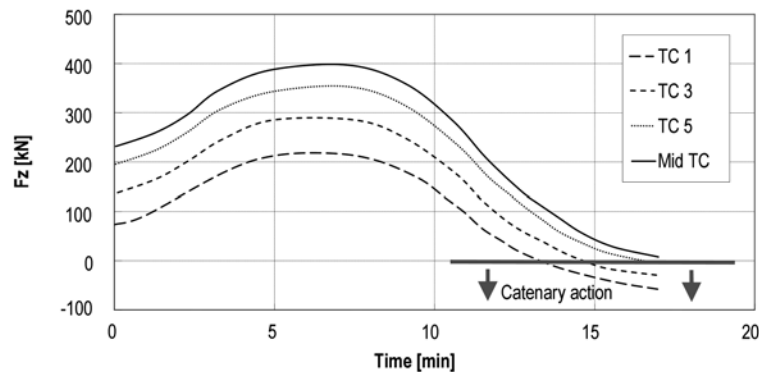


Fig. 14 Internal force variation along z-axis in top chord

occurred, the full capacity of the bottom chord is reached, although it has considerable ductility at this force level. Hence, with any further increase in temperature, the axial force within the member is seen to decrease as a result of the corresponding reduction in material strength. At 14.0 minutes (672 °C), the mid-span bottom chord section has effectively lost all bending resistance and also reaches its tensile capacity.

With respect to the top chord and slab performance, Fig. 14 reveals that, during the early period of the fire, the internal forces in the top chord and slab are considerably increased due to the thermal elongation. (this mechanism was also explained before for the protected models). However, once the mid-span section of the bottom chord reaches its flexural limit, the moment resistance of the composite truss, generated by the lever arm between top and bottom chords, is rapidly destroyed, and the internal forces of the top chord and slab reduced accordingly. Eventually, tensile force spreads across the composite, the top chord and slab from the ends towards the mid-span, allowing the composite girder to undergo full catenary action with horizontal support being provided by the columns (Fig. 12(c)). The supporting columns' contribution to the growth of catenary action can be interpreted from the change in direction of the horizontal reaction.

At 17.0 minutes, the second compressive web member (Fig. 15), which has previously been seen as sustaining the highest compressive load-ratio in the simply supported condition, is the first to buckle (Fig. 12(b)). Through a load redistribution process, resulting from the loss of stiffness of this web member, the compressive web member with the next-highest load-ratio is observed to buckle simultaneously. A

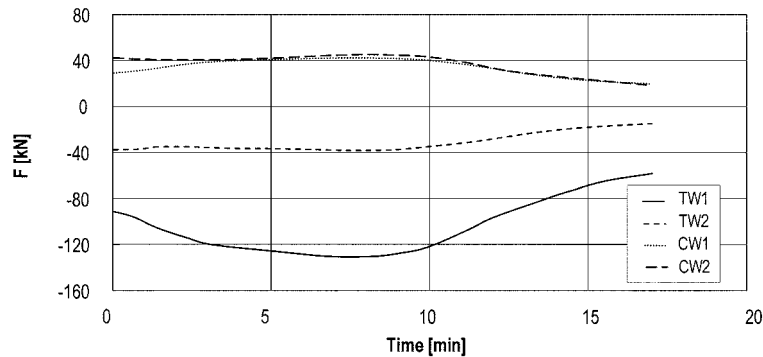


Fig. 15 Axial force variation in web members

series of progressive local instabilities then occurs from the ends of the truss towards the middle, causing much of the remaining part of the composite truss to lose its ability to resist catenary action.

The analyses have shown that the fire performance of the protected and unprotected composite trusses is not very sensitive to the level of loading considered, either in terms of deflection or of fire resistance period. If some residual protection were to remain on the composite trusses, the fire resistance period might be far more sensitive to the level of loading. If additional reinforcement were included in the slab, it might be possible for the slab and top chord to sustain catenary action for a long period after the buckling of the web members. However it is questionable whether or not the internal or external end-connections would be able to tolerate the sudden and massive change in horizontal reaction force brought about during the process of progressive collapse in the unprotected model when subjected to fire attack.

## 6. Conclusions

During the events of September 11<sup>th</sup> 2001, and as specified in their original design, the Twin Towers of the WTC maintained their integrity *via* load redistribution after experiencing initial structural damage due to airplane impact. However, under the resulting fire conditions, the buildings eventually collapsed. This study has been aimed towards contributing to understanding of the in-fire performance of long-span composite truss floor systems of the type employed in the WTC twin towers, with respect to the effects of passive protection, support conditions and loading.

Upper- and lower-bound cases of fire protection were considered; both two-hour protected and completely unprotected. In the unprotected cases, the temperatures of the individual truss elements were calculated using the incremental method given in Eurocode 4 Part 1.2 (European Committee for Standardisation 1994), on the basis of the section factor. The corresponding temperature distributions through the thickness of the slab were obtained from a detailed thermal analysis. For the protected case, the temperatures of truss members were assumed to increase to 200 °C as with the unprotected case, and then to develop linearly to 550 °C for the web members and 620 °C for the chords, at 120 minutes.

Using Vulcan, numerical analyses were conducted on composite trusses both with and without the restraint provided by supporting columns (representing the outer and middle floors among the fire exposed levels) for up to 60 minutes of the standard fire. These demonstrated that the unrestrained and protected composite truss, under both the 4.8 kN/m<sup>2</sup> and 3.9 kN/m<sup>2</sup> loadings, was able to resist 60

minutes of the standard fire with deflection below  $L/100$ . The unprotected simply supported trusses initially lost stability at 12.5 and 13.4 minutes due to the buckling of the second compressive web member. Conversely, the protected trusses with supporting columns deflected by approximately  $L/90$  (at 60 minutes of the standard fire) without experiencing any local member buckling. The unprotected composite truss was shown to resist 17.0 and 18.0 minutes of the standard fire before the progressive buckling of web members caused loss of stability. This would undoubtedly have re-stabilised when catenary action of the combined top chord and slab reinforcement took effect, but the tensile strength of these upper elements, together with tying strength of the beam-column connections, would then become critical. It was found that, for both types of support condition (with or without the columns), the fire resistance of the unprotected truss was relatively insensitive to the selected levels of loading. The degree of damage to the structure, or the extent of remaining passive fire protection in the high-load-carrying elements of the composite truss, was identified as crucial in determining the fire performance of the model.

Parameters such as the severity of the fire, the loading condition, the influence of the pattern of protection remaining after impact, and the connection robustness, need to be further investigated to understand the fire performance of the composite trusses in fire conditions.

## Acknowledgements

The authors gratefully acknowledge the support of METSEC Building Products Ltd, Korea Institute of Construction Technology and the collaboration of Buro Happold FEDRA.

## References

- American Society of Civil Engineering (1984), *Finite Element Analysis of Reinforced Concrete*, New York.
- Bailey, C.G. (1995), "Simulation of the structural behaviour of steel-framed buildings in fire", PhD thesis, University of Sheffield.
- Barzegar-Jamshidi, F. (1987), "Non-linear finite element analysis of reinforced concrete under short term monotonic loading", PhD thesis, University of Illinois at Urbana-Champaign, Ill.
- British Standards Institution (1990), BS.5950: Part8: Code of Practice for the Fire Protection of Structural Steelwork, UK.
- British Standards Institution (1996), BS.6399: Part1: Code of Practice for dead and imposed loads, UK.
- Cai, J. (2002), "Developments in modelling of composite building structures in fire", PhD thesis, University of Sheffield.
- Cai, J., Burgess, I.W., and Plank, R.J. (2003), "A generalised steel/reinforced beam-column element model for fire conditions", *Eng. Struct.*, **25**(6), 817-833.
- Choi, S.K. (2005), "The structural behaviour of composite truss systems in fire", PhD thesis, University of Sheffield.
- European Committee for Standardisation (1991), ENV 1991-1-2: Eurocode 1: Actions on Structures. Part1.2: General Actions: Actions on Structures Exposed to Fire, Brussels, BE.
- European Committee for Standardisation (1993), ENV 1993-1-2: Eurocode 3: Design of Steel Structures. Part1.2: General Rules: Structural Design for Fire, Brussels, BE.
- European Committee for Standardisation (1994), ENV 1994-1-2: Eurocode 4: Design of Composite Steel and Concrete Structures. Part 1.2: General Rules: Structural Fire Design, Brussels, BE.
- Federal Emergency Management Agency (2002), World Trade Center Building Performance Study: Data Collection, Preliminary Observations and Data Collections, Washington, DC.
- Fitzpatrick, T., Crane, R. and Rajii, A. (2002), "A briefing on the World Trade Center attacks", *Fire Protection*

- Engineering*, **13(Winter)**.
- Huang, Z., Platten, A. and Roberts, J. (1996), "Non-linear finite element model to predict temperature histories within reinforced concrete in fires", *Build. Environ.*, **31(2)**, 109-118.
- Huang, Z. and Platten, A. (1997), "Nonlinear finite element analysis of planar reinforced concrete members subjected to fire", *ACI Struct. J.*, **94(3)**, 272-282.
- Huang, Z., Burgess, I.W. and Plank, R.J. (2003), "Modelling membrane action of concrete slabs in composite buildings in fire I: Theoretical development", *ASCE J. Struct. Eng.*, **129a(8)**, 1093-1102.
- Huang, Z., Burgess, I.W. and Plank, R.J. (2003), "Modelling membrane action of concrete slabs in composite buildings in fire II: Validations", *ASCE J. Struct. Eng.*, **129b(8)**: 1103-1112.
- International Organization for Standardization (1975), ISO834: Fire resistance tests - Elements of building construction, Geneva.
- Milke, J. (2003), "Study of building performance in the WTC disaster", *Fire Protection Engineering*, **18(Spring)**.
- Najjar, S.R. (1994), "Three dimensional analysis of steel frames and sub-frames in fire", PhD thesis, University of Sheffield.
- Neville, A.M. (1998), *Properties of Concrete 4<sup>th</sup> edition*, Addition Wesley Longman Limited.
- Purkiss, J.A. (1996), *Fire Safety Engineering Design of Structures*, Butterworth & Heinemann, Oxford, UK.
- Ranby, A., Inha, T. and Myllymäki, J. (2000), *Structural Steel Fire Design*, SBI Publication 134, Sweden.
- Rots, J.G., Kusters, G.M.A. and Blaauwendraad, J. (1984), "The need for fracture mechanics options in finite element models for concrete structures", *Proc. Int. Conf. on Computer Aided Analysis and Design of Concrete Structures Part1*, Damjanic et al., eds., Pineridge Press, 19-32.
- Shepherd, P. (1999), "The performance in fire of restrained columns in steel-framed construction", PhD Thesis, University of Sheffield.

## Nomenclature

$A$	: exposed surface area of the steel cross section per unit length ( $\text{m}^2/\text{m}$ )
$C_a$	: specific heat of steel ( $600 \text{ J/kgK}$ )
$E_c(\theta)$	: $=1.5 f_c(\theta)/\varepsilon_{c1}(\theta)$
$F$	: member force (kN)
$f_s(\theta)$	: strength of steel in fire situation ( $\text{N/mm}^2$ )
$f_c(\theta)$	: compressive strength of concrete in fire situation ( $\text{N/mm}^2$ )
$f_t(\theta)$	: peak tensile strength of concrete in fire situation ( $\text{N/mm}^2$ )
$V$	: volume of the steel cross section per unit length ( $\text{m}^3/\text{m}$ )

## Greek letters

$\alpha_c$	: coefficient of convective heat transfer ( $25 \text{ W/m}^2\text{K}$ )
$\alpha_r$	: coefficient of radiative heat transfer ( $\text{W/m}^2\text{K}$ )
$\varepsilon_c(\theta)$	: concrete strain
$\varepsilon_{c1}(\theta)$	: concrete strain corresponding to $f_c(q)$
$\varepsilon_{ct}(\theta)$	: concrete strain corresponding to $f_t(q)$
$\varepsilon_{res}$	: resultant emissivity of the fire compartment and the heated surface
$\varepsilon_s(\theta)$	: steel strain
$\varepsilon_{ut}(\theta)$	: maximum tensile strain of concrete in fire situation
$\theta_i$	: average gas temperature during the interval $\Delta t$ ( $^\circ\text{C}$ )
$\theta_a$	: steel temperature at the end of the interval $\Delta t$ ( $^\circ\text{C}$ )
$\rho_a$	: density of steel ( $7850 \text{ kg/m}^3$ )
$\phi$	: configuration factor (conservatively taken as 1.0)

CC